



# Hydrogeochemical Processes Affecting Groundwater Chemistry in the Central Part of the Guanzhong Basin, China

Xiaofei Ren<sup>1,2</sup> · Peiyue Li<sup>1,2</sup> · Xiaodong He<sup>1,2</sup> · Fengmei Su<sup>1,2</sup> · Vetrimurugan Elumalai<sup>3</sup>

Received: 18 June 2020 / Accepted: 8 October 2020 / Published online: 4 November 2020  
© Springer Science+Business Media, LLC, part of Springer Nature 2020

## Abstract

Groundwater is essential for the sustainable development of the Guanzhong Basin, China, and its quality is mainly controlled by hydrogeochemical processes and anthropogenic pollution. This study used statistical and multivariate statistical analysis approaches to recognize the hydrogeochemical processes and affecting factors of groundwater in the central part of the Guanzhong Basin. Correlations among 14 hydrochemical parameters were statistically examined. Principal component analysis (PCA), factor analysis (FA), and hierarchical cluster analysis (HCA) techniques were applied to analyze the physicochemical variables to understand the affecting factors of groundwater quality in the study area. The correlation analysis results indicate that cation exchange is the dominant process affecting the concentration of  $\text{Na}^+$  and  $\text{Ca}^{2+}$  in the groundwater. Both the PCA and FA indicate that minerals dissolution/precipitation and human activities are the key factors that affect groundwater quality. All parameters except  $\text{CO}_3^{2-}$  and pH increase from C1 to C4 obtained through the Q mode HCA. C4 has a hydrochemical type of  $\text{SO}_4\text{--Na-K}$ , indicating that the sample of this cluster is primarily influenced by anthropogenic processes.

Groundwater resources have become an important resource for human survival, industrial development, and ecosystems (IAH 2015), especially in arid and semiarid regions. The high evaporation rate and limited precipitation in arid and semiarid regions make groundwater a valuable commodity in these regions (Li et al. 2015a). However, due to industrial and agricultural activities and unreasonable utilization of groundwater, some critical water sources have been seriously polluted with contaminants, such as fluoride, nitrate, arsenic, heavy metals, and synthetic organic compounds contaminants (Li et al. 2019a; Postigo and Barcelo 2015; Rodriguez-Lado et al. 2013; Soujanya et al. 2020). The inorganic cations and anions in groundwater could come from both natural and anthropogenic sources. Fendorf et al. (2010) showed that human activities can affect the release of

arsenic to groundwater, influencing the natural distribution of arsenic. Currently, groundwater quality deterioration has become a global problem impeding sustainable development (Li et al. 2017) and affecting human health (He and Wu 2019; He et al. 2019; Zhou et al. 2020a).

The Guanzhong Basin is located in the arid and semiarid area of Shaanxi Province, China. Limited surface water in this area makes groundwater the main source of drinking water in rural and isolated urban areas. With the implementation of the West Development Strategy of China and the Belt and Road Initiative, the economy of Guanzhong Basin has experienced rapid development. However, economic development has brought several challenges to groundwater resources, such as pollution, land desertification, and groundwater overexploitation (Han 2003; Wu et al. 2017). At present, the Guanzhong Basin plays a significant role in the Belt and Road Initiative, and the problem of water will become more severe as its implementation proceeds. Howard and Howard (2016) emphasized that the economic success of the Belt and Road Initiative in Central Asian countries hinges on a sound and sustainable management of water resources. A considerable amount of literature on groundwater pollution in the Guanzhong Basin has been published. Arsenic, nitrate, and fluoride are among the contaminants found in the groundwater in various areas across the Guanzhong Basin, all of which have an adverse influence

✉ Peiyue Li  
lipy2@163.com; peiyueli@chd.edu.cn

<sup>1</sup> School of Water and Environment, Chang'an University, No. 126 Yanta Road, Xi'an 710054, Shaanxi, China

<sup>2</sup> Key Laboratory of Subsurface Hydrology and Ecological Effects in Arid Region of the Ministry of Education, Chang'an University, No. 126 Yanta Road, Xi'an 710054, Shaanxi, China

<sup>3</sup> Department of Hydrology, University of Zululand, Kwa Dlangezwa, Durban 3886, South Africa

on human health (Li et al. 2014; Luo et al. 2014; Zhang et al. 2018). With the increased economic development, the safety of the water supply for human consumption is currently facing a great challenge in the Guanzhong Basin.

Because groundwater plays a crucial role in affecting economic development and anthropic activities in the Guanzhong Basin, rational development and utilization of groundwater are particularly important. Groundwater needs for human consumption, food production, energy, and environment have increased, which drives the development of water management globally (Gorelick and Zheng 2015). Several researchers have provided insights into water management. For example, an advanced agricultural irrigation method provided by Hu et al. (2010) can help to increase groundwater recovery and conserve agricultural water usage. Li et al. (2018a) proposed a rational and balanced groundwater and surface water utilization plan in the Yinchuan Plain, which provides new idea for water management in arid and semiarid areas. These studies describe novel ideas to decrease unreasonable and excessive water resource utilization and relieve the pressure of water management. However, efficient and effective groundwater management requires concerted efforts by the local authorities, scientists, and the public (Chen et al. 2018).

Groundwater contaminants affecting human health include fluoride, nitrate, organic matter, and microbial pathogens (Schwarzenbach et al. 2010; Ward et al. 2018). High fluoride levels in drinking water can cause dental and skeletal fluorosis (Kabir et al. 2019). Skin, lung, and bladder cancers, as well as hepatotoxicity and intellectual function impairment, are attributed to arsenic (Sun et al. 2011). Considering the consequences of water-quality deterioration, researchers are creating a database of known groundwater quality issues. Li et al. (2013a, b) conducted a comprehensive sensitivity analysis of the Technique for Order of Preference by Similarity to Ideal Solution (TOPSIS) method on water quality assessment, showing that the TOPSIS method is a feasible and reliable method for water-quality assessment. Adimalla et al. (2018) performed an assessment of groundwater quality focused on fluoride enrichment in a local area in India. Li et al. (2018b) performed groundwater quality assessment in the Loess Plateau, which determined the groundwater hydrochemical type and provided measures for sustainable groundwater quality management. Panneerselvam et al. (2020) applied GIS technology to evaluate the groundwater quality for domestic and irrigation purposes in hard rock region of India. Zhou et al. (2020b, c) assessed the groundwater quality for potable and irrigation usages and associated human health risks of two cities in North China Plain, providing scientific basis for sustainable groundwater utilization and protection. These studies promoted the development of groundwater quality assessments and provided

a foundation for household, agricultural, and industrial groundwater utilization.

To promote sustainable use of groundwater, groundwater quality and the hydrogeochemical processes controlling the groundwater quality should be studied to obtain a full understanding of fate of groundwater contaminants. Various groundwater pollution studies have been performed in Guanzhong Basin (Zhang et al. 2019; Luo et al. 2014). Most of these studies attribute the pollution to anthropogenic activities and local geological background. In addition, previous studies (Bu et al. 2010; Liu et al. 2003; Wu et al. 2020) have used multivariate statistical techniques, such as principal component analysis (PCA) or factor analysis (FA), to trace the affecting factor of groundwater pollution. In this study, PCA, FA, and hierarchical cluster analysis (HCA) were performed on groundwater geochemical measurements from the Guanzhong Basin and determine the hydrogeochemical processes affecting the major ion groundwater chemistry. This work aims to facilitate groundwater quality protection and management in the Guanzhong Basin area.

## Study Area

The Guanzhong Basin is located between east longitude 107° 30'–110° 30' and north latitude 34° 00'–35° 40'. It sits in an arid and semiarid climate zone with a cold and dry winter and a sweltering summer. The average annual rainfall is approximately 580 mm, with 60% concentrated in July through September. The unconsolidated deposits of the Guanzhong Basin consist of alluvial sediments and loess accumulation. With flat terrain, fertile soil, abundant water resource, and good irrigation condition, the Guanzhong Basin is one of the most productive areas in Shaanxi Province, China. Weihe River, the largest tributary of the Yellow River, runs through the Guanzhong Basin. However, this river is seriously pollution by industrial wastewater and domestic effluents, posing great risk on the groundwater quality in this area. The shallow groundwater level depth was approximately 2–20 m below the ground surface before the 1990s in these second terraces, and now it is 10–40 m in water level depth (Luo et al. 2014). The swift decline of groundwater level should be attributed to the heavy groundwater abstraction in this basin for domestic and industrial purposes, resulting in ground surface subsidence, and ground fissures.

The study area is located in the central part of the Guanzhong Basin, and it is the most important area for human population growth and economic development in the basin. In the study area, land use types can be classified into grassland, forest, surface water, agricultural land, urban land, unused land, and other construction land (covering 2.89%,

2.78%, 2.85%, 65.62%, 23.16%, 0.02%, and 2.68%, respectively, of the total study area) (Fig. 1).

Geologically, the study area is covered mainly by Quaternary sediments, which can be subdivided into four sublayers. From top down, they are the Holocene alluvial layer ( $Q_h^{al}$ ), the Upper Pleistocene alluvial layer ( $Q_{p3}^{al}$ ), the Middle Pleistocene layer ( $Q_{p2}^{al}$ ), and the Lower Pleistocene lacustrine layer ( $Q_{p1}^l$ ). The Holocene alluvial layer ( $Q_h^{al}$ ) is composed of coarse sand, medium-coarse sand, gravel sand, and silty clay and is mainly distributed in the Weihe River bed, floodplain, and first terrace areas. The Upper Pleistocene alluvial layer ( $Q_{p3}^{al}$ ) is distributed beneath the floodplain and the first terrace. The upper part of this layer is composed of gray-yellow silt and silty clay with a thickness of 15–25 m. The lower part is comprised by gray-white and gray-yellow medium-fine sand imbedded with silt and silty clay, ranging within 65–85 m in thickness. The Middle Pleistocene layer ( $Q_{p2}^{al}$ ) is mainly distributed in the floodplain and first terrace. The lithology of this layer is mainly medium-coarse sand and medium-fine sand with a thin layer of silty clay imbedded. The Lower Pleistocene lacustrine layer ( $Q_{p1}^l$ ) is composed of brown-yellow and gray-green silt, silty clay, and clay

imbedded with 5–10 sublayers of unstable gray–yellow and rusty yellow fine sand, medium-coarse sand.

In the study area, the confined aquifer and the phreatic aquifer are the main water supply aquifers (Zhou et al. 2018). The phreatic aquifer is composed of Middle Pleistocene to Holocene alluvial sand, gravel, and is separated from the confined aquifer by several layers of silty clay. The confined aquifer consists of Quaternary alluvial and lacustrine sand and gravel. The thickness of the phreatic aquifer is in general in the range of 20–90 m, and that of the confined aquifer is usually 60–180 m (Zhou et al. 2018). Groundwater levels continue to fall due to the exploitation of the phreatic aquifer and confined aquifer. Compared with the groundwater level before 2005, the groundwater levels of the confined aquifer have declined on average 20–40 m in the recent 10 years, with a maximum drop of more than 120 m (Tao et al. 2013). Therefore, a large cone of depression in the groundwater has been formed. In addition, due to the influence of climate change and human activities on groundwater, groundwater quality is degrading, and ecological environment problems are constraining the socio-economic development in the Guanzhong Basin (Wang et al. 2018). Atmospheric precipitation, river leakage, and irrigation

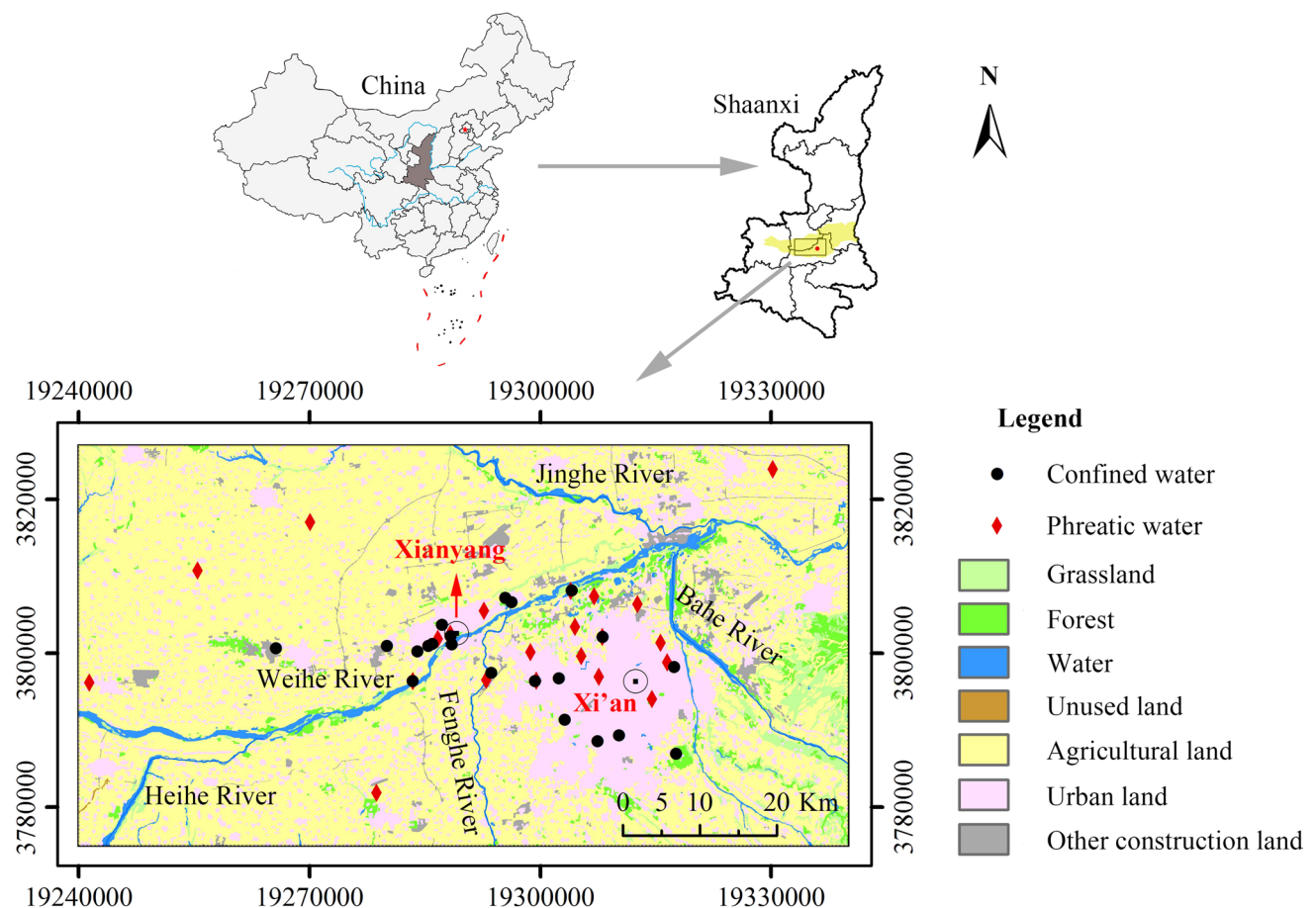


**Fig. 1** Location of the study area, land use/land cover, and groundwater sampling sites

infiltration are the main sources of groundwater recharge. In addition, lateral flow from the mountainous area also is a recharge source for groundwater. Regarding groundwater discharge, artificial abstraction, shallow groundwater evaporation, and lateral outflow are the main patterns of groundwater discharge.

## Methods

### Sample Collection and Analysis

Forty-four groundwater samples, including 22 samples (c1–c22) from the confined aquifer and 22 samples (q1–q22) from the phreatic aquifer, were collected in the study area of the Guanzhong Basin using polyethylene bottles (Fig. 1). Phreatic groundwater samples were collected from shallow wells with well depth ranging from 28 to 90 m. Confined groundwater samples were collected from deep wells with well depth ranging from 120 to 300 m. All of the wells belong to the regular monitoring wells monitored by local governmental institute. All bottles were washed three to four times with the groundwater to be collected before sampling. Water temperature and pH were directly measured in situ using portable, multiparameter devices (Hanna HI9811-5). After collection, the samples were sealed and stored at 4 °C until analysis.

Water samples were transported to the laboratory for measurement of physicochemical parameters, including major ions ( $\text{Na}^+$ ,  $\text{K}^+$ ,  $\text{Ca}^{2+}$ ,  $\text{Mg}^{2+}$ ,  $\text{HCO}_3^-$ ,  $\text{SO}_4^{2-}$ ,  $\text{Cl}^-$ , and  $\text{CO}_3^{2-}$ ), total dissolved solids (TDS), total hardness (TH), nitrate ( $\text{NO}_3^-$ ), fluoride ( $\text{F}^-$ ), and chemical oxygen demand (COD).  $\text{Na}^+$  and  $\text{K}^+$  were determined using flame atomic absorption spectrophotometry. Traditional titrimetric measured method used to determine  $\text{HCO}_3^-$  and  $\text{CO}_3^{2-}$ . EDTA titrimetric methods were adopted for analyzing  $\text{Ca}^{2+}$ ,  $\text{Mg}^{2+}$ , and TH.  $\text{NO}_3^-$  and  $\text{SO}_4^{2-}$  were analyzed by using spectrophotometer (ICS-1500) and  $\text{F}^-$  was tested by the ion-selective electrode method (ICS-90A). A standard solution of  $\text{AgNO}_3$  was used to determine the concentration of  $\text{Cl}^-$  in titration method. TDS was measured using drying and weighting approach. Dichromate method was used to analyze COD.

Duplicates were introduced during the testing to ensure the analytical accuracy in the experiment. Each sample was checked for accuracy using the ion charge balance error percentage (%CBE), as shown in Eq. (1). The results show that all samples have a %CBE less than  $\pm 5\%$  except sample c22 whose %CBE is  $-8.578\%$ . Therefore, sample c22 was not used in the study.

$$\% \text{CBE} = \frac{\text{TC} - \text{TA}}{\text{TC} + \text{TA}} \times 100 \quad (1)$$

where, TC and TA indicate the total concentrations of cations and anions, respectively. Both cations and anions are expressed in milliequivalent per liter (meq/L).

### Multivariate Statistical Techniques

Multivariate statistical techniques are widely used over the world in groundwater-quality studies to determine the sources and factors affecting the groundwater chemistry (Wu et al. 2014, 2020). Before using PCA, FA, and HCA, the original data were standardized by calculating the Z score for each measurement, which was performed using MATLAB 2016. The standardization procedure eliminated the influence of different units of measurement and created a dimensionless dataset. PCA and HCA were conducted using MATLAB 2016, and SPSS 24 was used to perform the correlation analysis and FA.

### Correlation Analysis

The physicochemical indices of the water were correlated by calculating the Pearson correlation coefficient ( $r$ ). The formula is expressed as:

$$r = \frac{\sum_i^n (x_i - \bar{x})(y_i - \bar{y})}{\sqrt{\sum_i^n (x_i - \bar{x})^2} \sqrt{\sum_i^n (y_i - \bar{y})^2}} \quad (2)$$

where  $r$  is the correlation coefficient between two variables ( $x$  and  $y$ ),  $\bar{x}$  and  $\bar{y}$  are the means of the variables. Before determining the correlation of  $x$  and  $y$ , the value of  $r$  should pass the significance test.

### Principal Component Analysis

PCA is a mathematical method of dimensionality reduction, which combines multiple indicators into a few indicators. PCA transforms the original variables into some integrated variables, called principal components (PCs) (Bu et al. 2010), and the PCs with the eigenvalues higher than one can be extracted (Cloutier et al. 2008). The PCs can be expressed by linear combinations (Wu et al. 2014):

$$y_i = c_{i1}x_1 + c_{i2}x_2 + \dots + c_{ip}x_p \quad (3)$$

where  $y$  is the PCs,  $c$  is the component loading,  $x$  is the origin variable,  $i$  is the component number and ranges from 1 to  $p$ , and  $p$  is the total number of variables.

## Factor Analysis

FA is generally conducted after PCA, and PCs are subjected to varimax rotation, generating varifactors (VFs). The FA can be expressed as Eq. (4).

$$x_i = a_{i1}f_1 + a_{i2}f_2 + \dots + a_{im}f_m + \varepsilon_i \quad (4)$$

where  $x$  is the original variables,  $a$  is the factor loading,  $f$  is the common factor,  $\varepsilon$  is the special factor,  $i$  is the variables number, and  $m$  is the total number of common factors. The common factors can be represented as linear combinations of the original variable, which is called factor score function, as shown in Eq. (5).

$$f_j = b_{j1}x_1 + b_{j2}x_2 + \dots + b_{jp}x_p \quad (5)$$

where  $f$  is the common factor,  $b$  is the variable loading,  $x$  is the origin variables,  $j$  is the common factor number, and  $p$  is the origin variables number.

## Hierarchical Cluster Analysis

HCA is a multivariate statistical technique that can classify samples (Q mode HCA) or variables (R mode HCA) based on their similarity (Vega et al. 1998). In this study, both Q mode and R mode HCA were used with the Ward linkage rule and Euclidean distance to classify different clusters. The results of HCA are shown as a dendrogram, which can clearly explain the classification of the data.

## Results and Discussion

### Hydrochemical Characteristics

Groundwater hydrochemical characteristics are very complex and depend on multiple factors, such as weathering of rocks, cation exchange, recharge water quality, river water leakage, evaporation, and anthropogenic factors (Li et al. 2018b). To interpret the hydrochemistry of the groundwater in the study area, the statistical properties of the groundwater hydrochemical data are listed in Table 1.

The pH value of the groundwater ranges from 7.56 to 8.74, indicating alkaline groundwater in nature. The concentrations of TDS and TH range from 96.00 to 3400.00 mg/L and 73.84 to 1214.00 mg/L, respectively. Groundwater TH in the study area varied greatly (confined water 73.84–572.00 mg/L, phreatic water 95.13–1214.00 mg/L). In the hydrogeological environment, confined water and phreatic water have different impact factors, resulting in the differences in the groundwater hydrochemistry between the two sources. As shown in Table 1, the concentration

of  $\text{Na}^+$  ranges from 2.09 to 339.00 mg/L with a mean of 117.74 mg/L in the confined water, whereas that in the phreatic water varies from 17.30 to 706.00 mg/L with a mean of 149.35 mg/L. The concentration of  $\text{Mg}^{2+}$  ranges from 2.02 to 82.32 mg/L in the confined water, but in the phreatic water it varies from 6.06 to 254.30 mg/L. The other ions ( $\text{K}^+$ ,  $\text{Ca}^{2+}$ ,  $\text{F}^-$ ,  $\text{Cl}^-$ ,  $\text{SO}_4^{2-}$ ,  $\text{HCO}_3^-$ , and  $\text{NO}_3^-$ ) have similar trends that the concentrations in the confined water are lower than those in the phreatic water. The cause of this phenomenon is that the phreatic water is more susceptible to pollution compared with the confined water.

Particularly, the mean concentration of  $\text{SO}_4^{2-}$  in the phreatic water is 479.05 mg/L in the agricultural land (q8, q9, q18, q19) and the mean concentration of  $\text{NO}_3^-$  is 57.21 mg/L, both of which are much higher than the average concentrations of  $\text{SO}_4^{2-}$  and  $\text{NO}_3^-$  in phreatic water (191.87 mg/L and 23.33 mg/L, respectively). However, there is an opposite finding for the concentration of COD. The high concentration of  $\text{SO}_4^{2-}$  and  $\text{NO}_3^-$  in the phreatic may be attributed to the utilization of pesticides and fertilizers in the agricultural land and high groundwater level contributing to high groundwater evaporation. Groundwater with high COD level is concentrate in the urban land and other construction land. It can be inferred that the domestic and industrial sewage lead to the high concentration of COD.

A Piper diagram (Piper 1944) was used to study the hydrochemical types of groundwater. As shown in Fig. 2, most of the confined water and phreatic water samples are classified as  $\text{HCO}_3\text{-Na}$  or  $\text{HCO}_3\text{-Ca}\cdot\text{Mg}$  types, and several water samplings can be classified as  $\text{SO}_4\cdot\text{Cl-Ca}\cdot\text{Mg}$  or  $\text{SO}_4\cdot\text{Cl-Na}$  types. The anions were plotted mainly in zones B (No dominant type) and E (Bicarbonate type). The cations, however, fall into the zones B (No dominant type) and D (Sodium type). The triangle in lower left corner suggest that alkali mental has the advantage over alkali earth mental. The high sodium concentration may come from cation exchange and water percolation which introduces sodium from vadose zone into groundwater. The high concentration of  $\text{HCO}_3^-$ , as indicated by the lower right triangle, shows that carbonate dissolution is an important process regulating the major anions. The observation of Piper diagram shows that groundwater chemistry may be regulated by the water–rock interaction and rock weathering.

Gibbs diagrams are a widely used tool for understanding the natural formation mechanism of groundwater. There are three mechanisms according to the Gibbs diagram: evaporation dominance, rock dominance, and precipitation dominance. Figure 3 shows that most of the water samples are plotted in the middle section of the diagrams. This observation suggests that rock weathering is the most significant natural mechanism governing the groundwater evolution in the study area. The dissolution of minerals and salts, such as calcite, dolomite, and halite, enter the

**Table 1** Major physicochemical indices of the groundwater in the study area

Parameters	Units	Minimum		Maximum		Mean		Standard deviation		National standards		NSBL <sup>a</sup>	
		Confined water	Phreatic water	Confined water	Phreatic water	Confined water	Phreatic water	Confined water	Phreatic water	Confined water	Phreatic water	Confined water	Phreatic water
pH	–	7.76	7.56	8.67	8.74	8.31	8.22	0.23	0.30	6.5–8.5	5	4	
K <sup>+</sup>	mg/L	0.46	0.55	6.41	9.50	1.81	2.03	1.59	2.05	–	–	–	
Na <sup>+</sup>	mg/L	2.09	17.30	339.00	706.00	117.74	149.35	77.23	151.89	200	2	3	
Ca <sup>2+</sup>	mg/L	17.00	11.30	126.00	122.80	42.08	57.63	24.17	27.87	–	–	–	
Mg <sup>2+</sup>	mg/L	2.02	6.06	82.32	254.30	31.33	59.19	23.81	52.10	–	–	–	
F <sup>-</sup>	mg/L	0.10	0.01	1.95	2.36	0.66	0.77	0.47	0.59	1.0	3	4	
Cl <sup>-</sup>	mg/L	5.19	12.26	279.00	569.20	70.31	107.29	69.57	120.10	250	1	1	
SO <sub>4</sub> <sup>2-</sup>	mg/L	5.35	7.41	345.00	1204.00	110.90	191.87	86.80	246.33	250	2	6	
HCO <sub>3</sub> <sup>-</sup>	mg/L	70.00	198.60	572.00	947.10	336.15	425.78	139.40	180.64	–	–	–	
CO <sub>3</sub> <sup>2-</sup>	mg/L	0.00	0.00	17.20	25.90	5.96	3.98	6.34	7.10	–	–	–	
NO <sub>3</sub> <sup>-</sup>	mg/L	0.25	0.12	51.62	161.50	8.12	23.33	14.35	41.73	20	3	6	
TDS	mg/L	96.00	267.00	1128.00	3400.00	591.43	829.91	282.17	659.05	1000	2	5	
COD	mg/L	0.28	0.28	4.00	6.58	0.92	1.17	0.80	1.26	3	1	1	
TH	mg/L	73.84	124.80	572.00	1214.00	234.14	389.17	140.46	232.21	450	3	9	

<sup>a</sup>Number of samples beyond the national standards

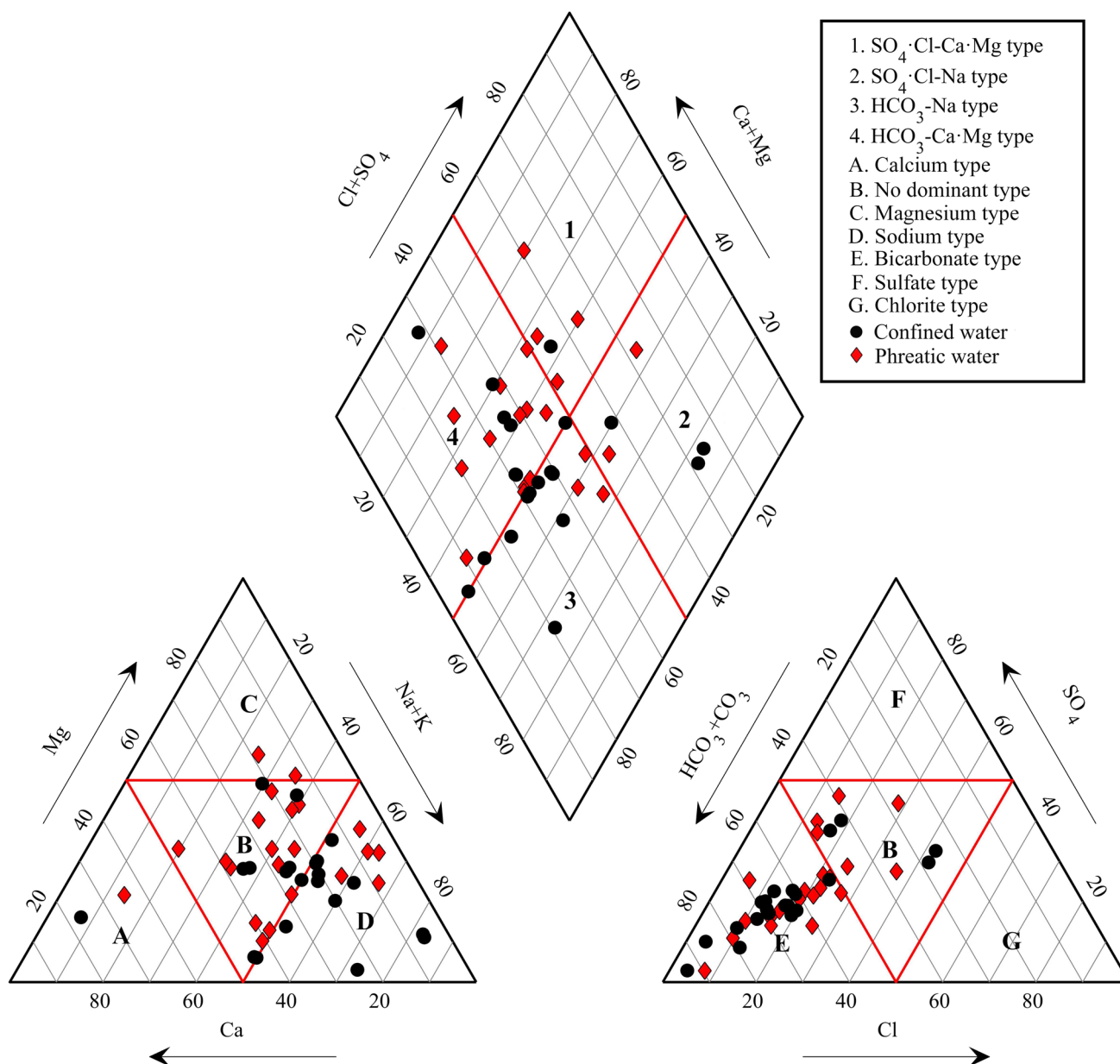


Fig. 2 Piper diagram showing the hydrochemical characteristics of phreatic water and confined water

groundwater through water–rock interactions. Figure 3 also shows that the phreatic water has a greater tendency for evaporation compared to the confined water. This is indicative of phreatic groundwater in an arid and semiarid area being typically subjected to greater evaporation compared with deeper subsurface water sources. Therefore, it is evident that phreatic water geochemistry in the study area is conjunctively influenced by major rock weathering and slight evaporation. However, the Piper diagram and Gibbs diagrams are only capable of analyzing the natural process. The anthropogenic processes should be evaluated by other techniques for further study.

### Correlation Analysis

Forty-three samples with 14 physicochemical indices were used in the correlation analysis, resulting in a correlation coefficient matrix shown in Table 2.  $\text{Cl}^-$  significantly correlates to  $\text{Na}^+$  ( $r=0.944$ ,  $p < 0.01$ ), which implies that the dissolution of halite is a possible source of both  $\text{Na}^+$  and  $\text{Cl}^-$ . The relationship between  $\text{Na}^+$  and  $\text{Cl}^-$  also were plotted in Fig. 4a, which suggests that there are additional sources for  $\text{Na}^+$ , because it is not a 1:1 relationship between the two ions. The dissolution of dolomite and calcite are the primary sources of  $\text{Ca}^{2+}$ ,  $\text{Mg}^{2+}$ ,

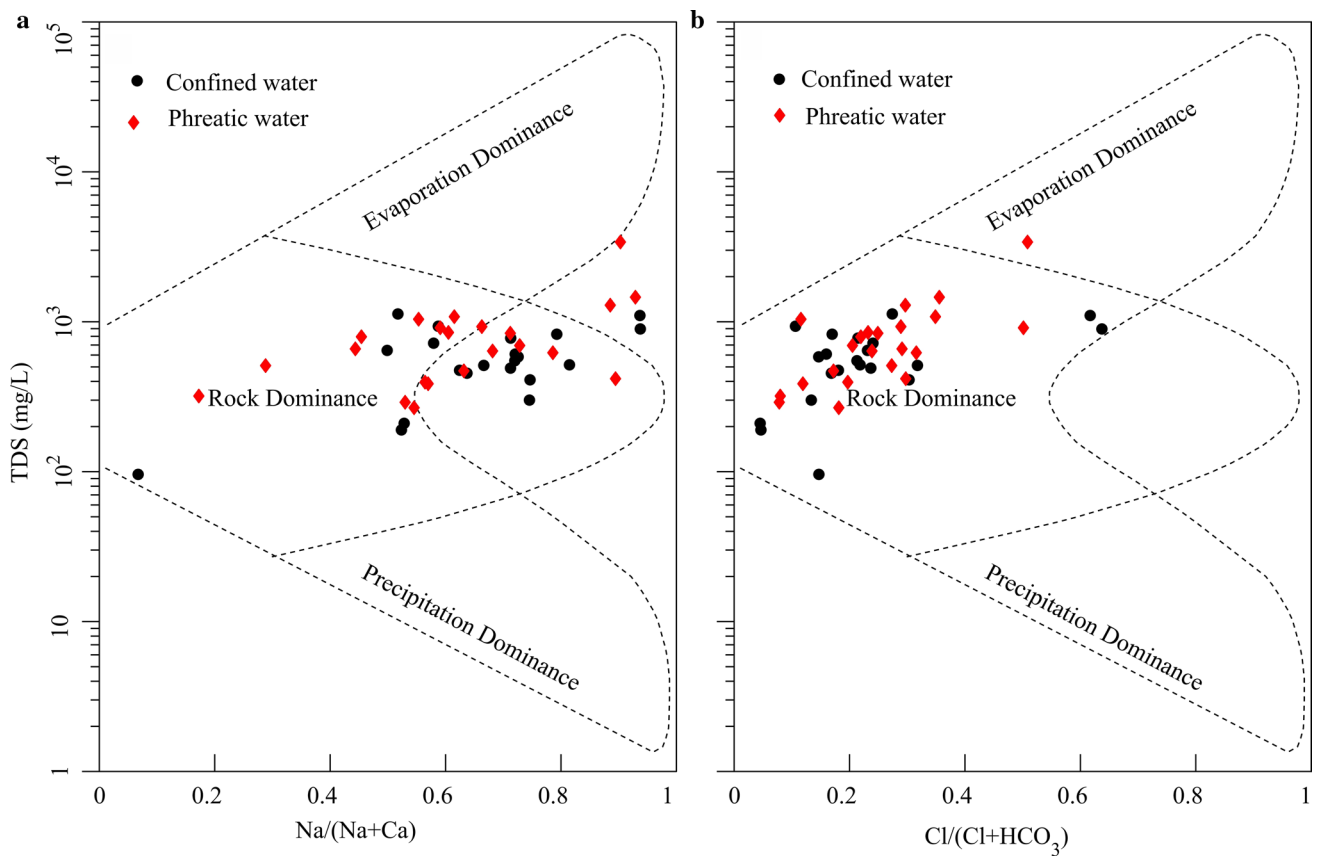


Fig. 3 Gibbs diagrams of the confined water and phreatic water

Table 2 Matrix of correlation coefficients for the 14 water quality variables from the Guanzhong Basin

	pH	K <sup>+</sup>	Na <sup>+</sup>	Ca <sup>2+</sup>	Mg <sup>2+</sup>	F <sup>-</sup>	Cl <sup>-</sup>	SO <sub>4</sub> <sup>2-</sup>	HCO <sub>3</sub> <sup>-</sup>	CO <sub>3</sub> <sup>2-</sup>	NO <sub>3</sub> <sup>-</sup>	TDS	COD	TH
pH	1	-0.278	0.136	<b>-0.727</b>	-0.130	<b>0.392</b>	0.006	-0.122	-0.081	<b>0.623</b>	-0.174	-0.068	-0.288	<i>-0.345</i>
K <sup>+</sup>		1	<b>0.445</b>	0.261	<b>0.494</b>	0.085	<b>0.452</b>	<b>0.611</b>	<i>0.357</i>	-0.280	0.263	<b>0.609</b>	<b>0.408</b>	<b>0.506</b>
Na <sup>+</sup>			1	-0.028	<b>0.758</b>	<b>0.725</b>	<b>0.944</b>	<b>0.895</b>	<b>0.732</b>	0.077	<i>0.362</i>	<b>0.901</b>	-0.052	<b>0.638</b>
Ca <sup>2+</sup>				1	0.285	-0.329	0.112	0.288	0.265	<b>-0.407</b>	0.269	0.201	0.278	<b>0.568</b>
Mg <sup>2+</sup>					1	<b>0.519</b>	<b>0.797</b>	<b>0.853</b>	<b>0.878</b>	-0.065	<b>0.659</b>	<b>0.882</b>	-0.009	<b>0.950</b>
F <sup>-</sup>						1	<b>0.654</b>	<b>0.505</b>	<b>0.548</b>	0.294	0.224	<b>0.567</b>	-0.181	<i>0.341</i>
Cl <sup>-</sup>							1	<b>0.906</b>	<b>0.666</b>	-0.064	<b>0.466</b>	<b>0.903</b>	-0.040	<b>0.717</b>
SO <sub>4</sub> <sup>2-</sup>								1	<b>0.711</b>	-0.128	<b>0.424</b>	<b>0.925</b>	0.128	<b>0.822</b>
HCO <sub>3</sub> <sup>-</sup>									1	0.064	<b>0.463</b>	<b>0.793</b>	-0.104	<b>0.838</b>
CO <sub>3</sub> <sup>2-</sup>										1	-0.104	-0.038	-0.332	-0.178
NO <sub>3</sub> <sup>-</sup>											1	<b>0.505</b>	-0.009	<b>0.656</b>
TDS												1	0.036	<b>0.819</b>
COD													1	0.081
TH														1

Bold values represent a correlation that is significant at the 0.01 level (two-tailed)

Italic values represent a correlation that is significant at the 0.05 level (two-tailed)

and HCO<sub>3</sub><sup>-</sup>, so these ions should have a high correlation and HCO<sub>3</sub><sup>-</sup> versus (Ca<sup>2+</sup> + Mg<sup>2+</sup>) should be in a theoretical range (Li et al. 2016a). Table 2, however, shows that

the correlation coefficient between Ca<sup>2+</sup> with HCO<sub>3</sub><sup>-</sup> is insignificant. Figure 4c shows that (Ca<sup>2+</sup> + Mg<sup>2+</sup>) versus



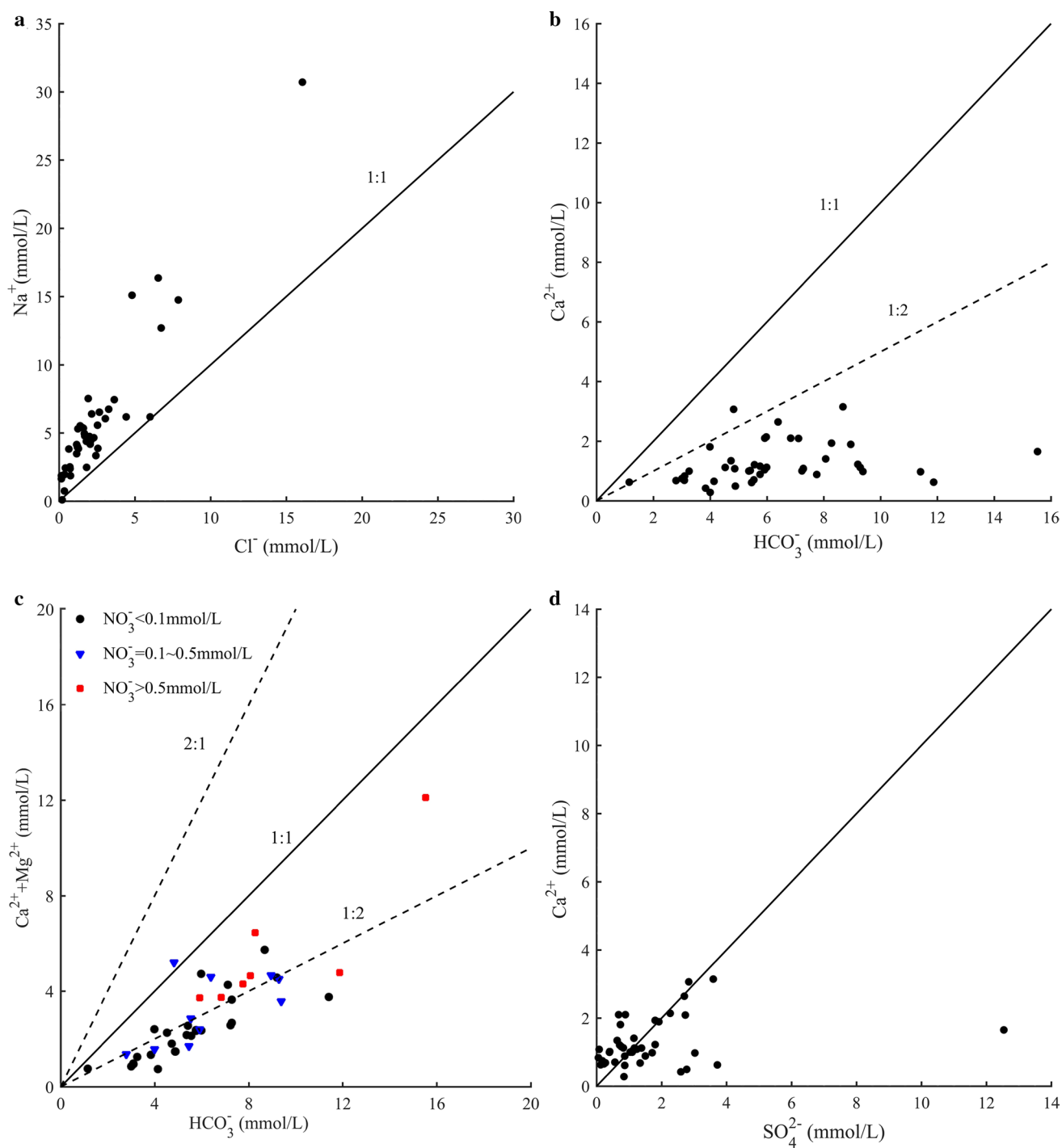


**Fig. 4** Plots of **a**  $\text{Na}^+$  versus  $\text{Cl}^-$ , **b**  $\text{Ca}^{2+}$  versus  $\text{HCO}_3^-$ , **c**  $\text{Ca}^{2+} + \text{Mg}^{2+}$  versus  $\text{HCO}_3^-$  and **d**  $\text{Ca}^{2+}$  versus  $\text{SO}_4^{2-}$

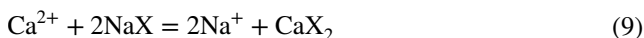
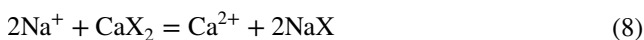
$\text{HCO}_3^-$  does not plot within the theoretical range. This discrepancy could be attributed to the cation exchange between  $\text{Ca}^{2+}$  and  $\text{Na}^+$  in the groundwater. Schoeller (1965) proposed two chloro-alkaline indices (CAI-1 and

CAI-2) for the study of cation exchange. They are defined as (Li et al. 2014):

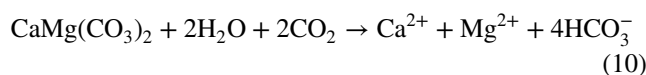
$$\text{CAI} - 1 = \frac{\text{Cl}^- - (\text{Na}^+ + \text{K}^+)}{\text{Cl}^-} \quad (6)$$

$$\text{CAI} - 2 = \frac{\text{Cl}^- - (\text{Na}^+ + \text{K}^+)}{\text{HCO}_3^- + \text{SO}_4^{2-} + \text{CO}_3^{2-} + \text{NO}_3^-} \quad (7)$$

As expressed in Eq. (8), positive values for the two indices indicate cation exchange, whereas negative values indicate reverse ion exchange as expressed as Eq. (9) (Li et al. 2016b). There are 97.67% samples with negative CAI-1 and CAI-2, and only one sample with positive values. Thus, cation exchange expressed in Eq. (9) is the important process controlling the groundwater chemistry. To confirm the occurrence of cation exchange reaction, the bivariate diagram of  $(\text{Ca}^{2+} + \text{Mg}^{2+}) - (\text{HCO}_3^- + \text{SO}_4^{2-})$  as a function of  $(\text{Na}^+ + \text{K}^+ - \text{Cl}^-)$  in Fig. 5b shows a slope of  $-1$ , indicating, again, the existence of a cation–anion exchange phenomenon.



The concentration of  $\text{CO}_2$  in water controls the dissolution of calcite and dolomite in the groundwater (Li et al. 2016a). As shown in Fig. 4b and c, molarity ratio of  $\text{Ca}^{2+} + \text{Mg}^{2+}$  versus  $\text{HCO}_3^-$  is close to 1:2, indicating that there are other processes influencing  $\text{Ca}^{2+}$  concentration. The dissolution of dolomite can be expressed as Eq. (10):



Li et al. (2015b, 2019a, b) and Dar et al. (2011) have comprehensively explored fluoride and nitrate concentrations in groundwater, because these two contaminants have great impacts on groundwater quality and human health. As shown in Table 2,  $\text{F}^-$  has a significant correlation with pH and  $\text{HCO}_3^-$  ( $r=0.392$  and  $r=0.548$  at a significance level of  $p < 0.01$ , respectively), which indicates that the alkaline nature of water is more favorable for fluoride enrichment. Similarly, Li et al. (2014) and Adimalla et al. (2018) adopted some chemical reactions to explain the sources of fluoride in the groundwater and obtained the same conclusion about fluoride enrichment. There is a positive correlation between  $\text{F}^-$  and  $\text{Na}^+$  ( $r=0.725$  at a significance level of  $p < 0.01$ ) in Table 2, which implies that the high concentration of  $\text{Na}^+$  will favor the enrichment of  $\text{F}^-$  in groundwater. Wu et al. (2020), Panneer et al. (2017), and Hossain et al. (2016) gained a similar finding about fluoride enrichment. The molar concentration of  $(\text{Ca}^{2+} + \text{Mg}^{2+})$  and  $\text{HCO}_3^-$  are plotted in Fig. 4c, which indicates that with the increased concentration of  $\text{NO}_3^-$ , the molarity ratio of  $(\text{Ca}^{2+} + \text{Mg}^{2+})$  versus  $\text{HCO}_3^-$  tends to increase. Human activities contribute heavily to the concentration of nitrate in the groundwater (Bouchard et al. 1992). Hence anthropogenic processes may accelerate the release of  $\text{Ca}^{2+}$  and  $\text{Mg}^{2+}$  from the surrounding minerals.

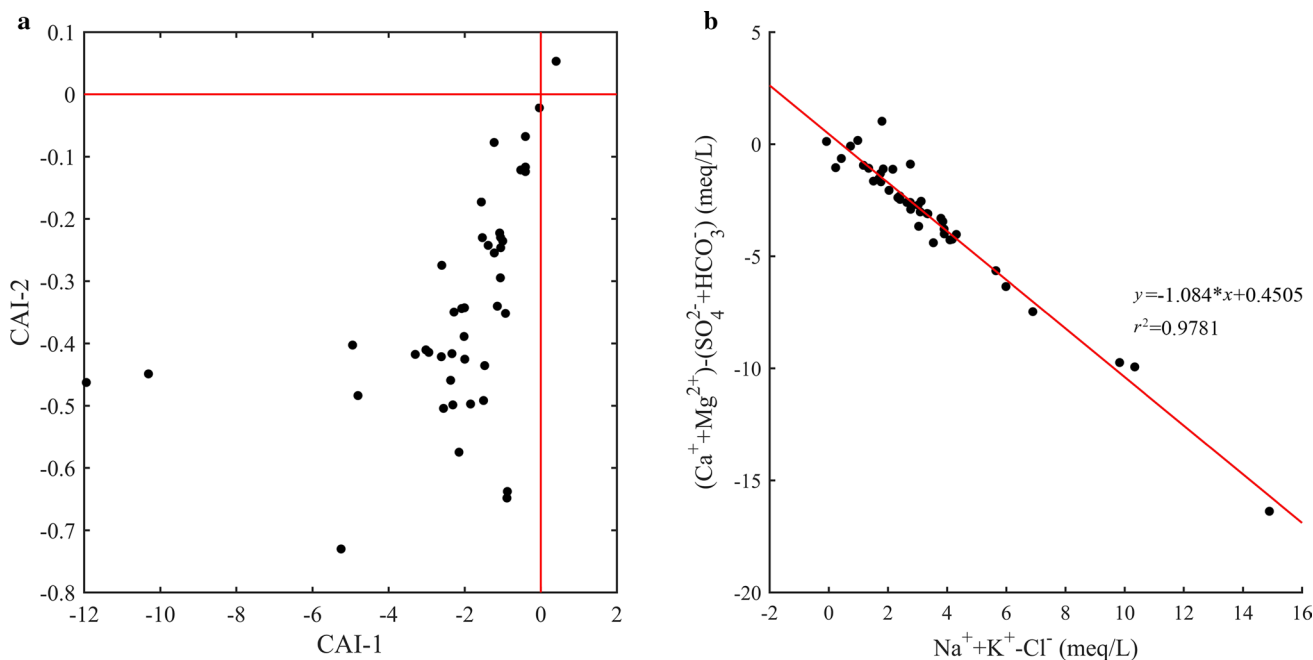


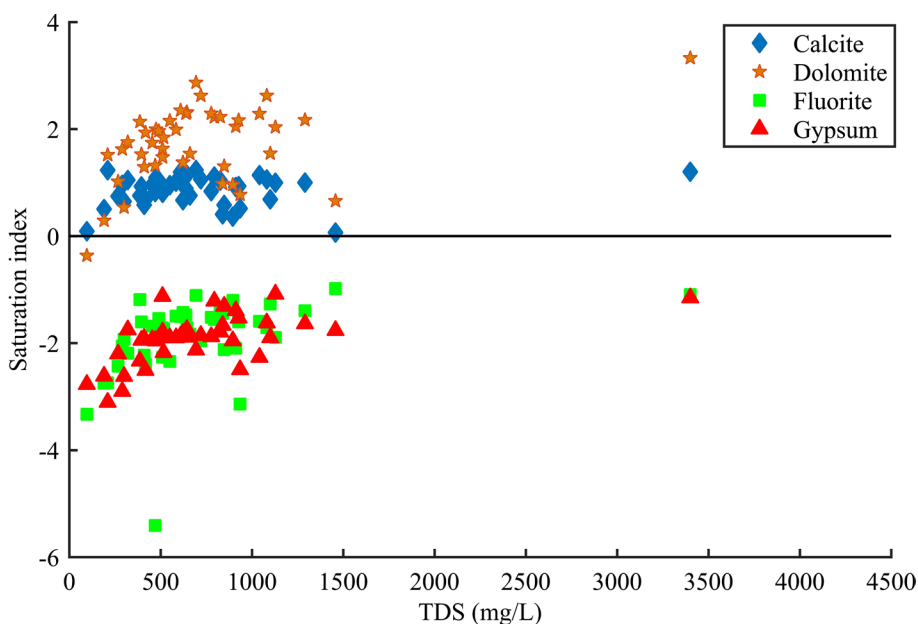
**Fig. 5** Plots of **a** CAI-1 versus CAI-2 and **b**  $(\text{Ca}^{2+} + \text{Mg}^{2+}) - (\text{SO}_4^{2-} + \text{HCO}_3^-)$  against  $\text{Na}^+ + \text{K}^+ - \text{Cl}^-$

Gypsum is a potential source of  $\text{Ca}^{2+}$  and  $\text{SO}_4^{2-}$  in the area, but the correlation coefficient of them is insignificant ( $r=0.288$ ). Figure 4d displays the concentration relationship between  $\text{Ca}^{2+}$  and  $\text{SO}_4^{2-}$ , indicating that  $\text{Ca}^{2+}$  and  $\text{SO}_4^{2-}$  are from other sources in addition to gypsum. Shown by Table 2,  $\text{SO}_4^{2-}$  is positively correlated with  $\text{NO}_3^-$  ( $r=0.424$  at a significance level of  $p<0.01$ ), indicating that anthropogenic factors may be an important source of  $\text{SO}_4^{2-}$ .

Generally, TDS and TH should be significantly correlated with major ions. TDS is significantly correlated with  $\text{K}^+$ ,  $\text{Na}^+$ ,  $\text{Mg}^{2+}$ ,  $\text{F}^-$ ,  $\text{Cl}^-$ ,  $\text{SO}_4^{2-}$ ,  $\text{HCO}_3^-$ , and  $\text{NO}_3^-$  ( $r=0.609, 0.901, 0.882, 0.567, 0.903, 0.925, 0.793$ , and  $0.505$ , respectively, at significance level of  $p<0.01$ ). Table 2 shows that TH is significantly correlated to  $\text{Ca}^{2+}$ ,  $\text{Mg}^{2+}$ ,  $\text{Cl}^-$ ,  $\text{SO}_4^{2-}$ ,  $\text{HCO}_3^-$ , and  $\text{NO}_3^-$  ( $r=0.568, 0.950, 0.717, 0.822, 0.838$ , and  $0.656$ , respectively, at significance level of  $p<0.01$ ).

Saturation indices (SI) are usually used to describe the dissolution/precipitation of minerals in the groundwater (Li et al. 2010). The saturation indices of calcite, dolomite, fluorite, and gypsum at 25 °C were calculated via PHREEQC (Parkhurst and Appelo 1999) and plotted in Fig. 6 as a function of TDS. SI of fluorite and gypsum are both negative, which indicates that fluorite and gypsum are undersaturated in the groundwater and more fluorite and gypsum can dissolve into the groundwater under suitable conditions. The saturation indices of calcite and dolomite, however, are positive, except one sample, which indicates that calcite and dolomite tend to precipitate in the groundwater. With the increasing trend of TDS, the saturation indices of fluorite and gypsum slightly increase, which may cause the precipitation of calcite and dolomite.

**Fig. 6** Relationships of saturation indices of calcite, dolomite, fluorite, and gypsum with TDS



## Principal Component Analysis and Factor Analysis

The number of components in PCA is determined by the Kaiser criterion, for which the components with eigenvalues greater than 1 are retained. As shown in Table 3a, the first three principal components (PCs) have eigenvalues greater than 1, and they represent 79.281% of the total variance in the hydrochemistry dataset. Table 3a presents the principal component loadings for these components, which shows the importance of the variables for each component. The component loadings can be classified as strong, moderate, and weak based on the absolute loading values of  $>0.75$ ,  $0.75-0.5$ , and  $0.50-0.30$ , respectively (Bu et al. 2010; Liu et al. 2003).

PC1 explains 50.423% of the total variance, and it has strong loadings on  $\text{Na}^+$ ,  $\text{Mg}^{2+}$ ,  $\text{Cl}^-$ ,  $\text{SO}_4^{2-}$ ,  $\text{HCO}_3^-$ , TDS, and TH (0.884, 0.951, 0.908, 0.942, 0.853, 0.961, and 0.913, respectively), and moderate loadings on  $\text{K}^+$ ,  $\text{F}^-$ , and  $\text{NO}_3^-$  (0.591, 0.580, and 0.603, respectively). PC1 can be regarded as the salinity component of the water. TDS and TH have high loadings in PC1, because TDS and TH are significantly correlated with most ions (Table 2).  $\text{Na}^+$ ,  $\text{K}^+$ ,  $\text{Mg}^{2+}$ ,  $\text{Cl}^-$ ,  $\text{HCO}_3^-$ , and  $\text{F}^-$  are the important indices contributing to salinity and mainly come from weathering and dissolution of halite, dolomite, and fluorite. As discussed previously,  $\text{NO}_3^-$  and  $\text{SO}_4^{2-}$  are closely related to the anthropogenic processes. Therefore, PC1 represents a mixture of natural and anthropogenic processes.

PC2 and PC3 explain 20.836% and 8.562% of the total variance, respectively, which indicates that PC2 and PC3 are secondary factors. PC2 is characterized by strong loadings on pH and  $\text{Ca}^{2+}$  (0.864 and  $-0.779$ , respectively) and moderate loadings on  $\text{F}^-$  and  $\text{CO}_3^{2-}$  (0.634

**Table 3** Total variance explained by (a) PC and the loading matrix of PCs, (b) VF and the loading matrix of VFs

Variables	Components				
	1	2	3		
(a)					
pH	-0.149	<b>0.864</b>	0.168		
K <sup>+</sup>	<b>0.591</b>	-0.345	0.496		
Na <sup>+</sup>	<b>0.884</b>	0.330	0.192		
Ca <sup>2+</sup>	0.305	<b>-0.779</b>	-0.305		
Mg <sup>2+</sup>	<b>0.951</b>	0.003	-0.165		
F <sup>-</sup>	<b>0.580</b>	<b>0.634</b>	0.098		
Cl <sup>-</sup>	<b>0.908</b>	0.184	0.116		
SO <sub>4</sub> <sup>2-</sup>	<b>0.942</b>	-0.015	0.179		
HCO <sub>3</sub> <sup>-</sup>	<b>0.853</b>	0.104	-0.240		
CO <sub>3</sub> <sup>2-</sup>	-0.101	<b>0.725</b>	-0.158		
NO <sub>3</sub> <sup>-</sup>	<b>0.603</b>	-0.132	-0.395		
TDS	<b>0.961</b>	0.079	0.101		
COD	0.056	-0.529	<b>0.635</b>		
TH	<b>0.913</b>	-0.247	-0.246		
Eigenvalue	7.059	2.917	1.199		
% of variance	50.423	20.836	8.562		
Cumulative %	50.423	71.259	79.821		
Variables	Components				
	1	2	3	4	5
(b)					
pH	0.021	<b>-0.782</b>	-0.132	-0.053	0.463
K <sup>+</sup>	0.497	0.154	<b>0.666</b>	0.050	-0.151
Na <sup>+</sup>	<b>0.959</b>	-0.175	0.040	0.031	-0.002
Ca <sup>2+</sup>	0.112	<b>0.916</b>	0.142	0.114	-0.091
Mg <sup>2+</sup>	<b>0.849</b>	0.205	0.042	0.418	0.055
F <sup>-</sup>	<b>0.706</b>	-0.464	-0.159	0.057	0.140
Cl <sup>-</sup>	<b>0.935</b>	-0.079	0.022	0.137	-0.144
SO <sub>4</sub> <sup>2-</sup>	<b>0.928</b>	0.129	0.210	0.084	-0.077
HCO <sub>3</sub> <sup>-</sup>	<b>0.818</b>	0.263	-0.095	0.218	0.226
CO <sub>3</sub> <sup>2-</sup>	0.010	-0.321	-0.186	-0.046	<b>0.890</b>
NO <sub>3</sub> <sup>-</sup>	0.340	0.106	0.016	<b>0.919</b>	-0.063
TDS	<b>0.938</b>	0.070	0.151	0.183	-0.003
COD	-0.084	0.134	<b>0.901</b>	-0.002	-0.103
TH	<b>0.761</b>	0.473	0.081	0.402	0.028
Eigenvalue	6.389	2.215	1.440	1.314	1.153
% of variance	45.638	15.821	10.288	9.382	8.237
Cumulative %	45.638	61.459	71.747	81.129	89.366

Bold values indicate high loadings of PCs or VFs on variables

and 0.725, respectively). The positive loadings on pH, F<sup>-</sup>, and CO<sub>3</sub><sup>2-</sup> and negative loadings on Ca<sup>2+</sup> precisely correspond to the correlation between these ions (Table 2). Some researchers have found that an alkaline environment is conducive to the enrichment of fluoride and obstructs the dissolution of calcite and dolomite. PC2 represents fluorite dissolution and can be indicative of natural process. PC3

has a moderate loading on COD (0.635) and is deemed as the organic matter component. COD is mainly from human activity. Therefore, PC3 represents anthropogenic processes.

The difference between PCA and FA is that the FA must undergo a rotation process on the basis of PCA. The first five varifactors (VFs) in the factor analysis explain 89.366% of the total variance. As shown in Table 3a, b, the VF1 is

consistent with PC1, representing salinity component of water. VF2 has a strong positive loading on  $\text{Ca}^{2+}$  and strong negative loading on pH, which represent the release of calcium into the groundwater. VF3 is the consistent with PC3, representing anthropogenic processes. VF4 has a strong positive loading on  $\text{NO}_3^-$  (0.919), which represents the nitrate process in the water. VF5 has a strong loading on  $\text{CO}_3^{2-}$  (0.890), indicating that carbonate process is significant in the Guanzhong Basin groundwater. As describe above, both PCA and FA could be used to analyze the main factors affecting groundwater hydrochemical characteristics. Compared with PCA, FA is more accurate in the interpretation of results.

### Hierarchical Cluster Analysis

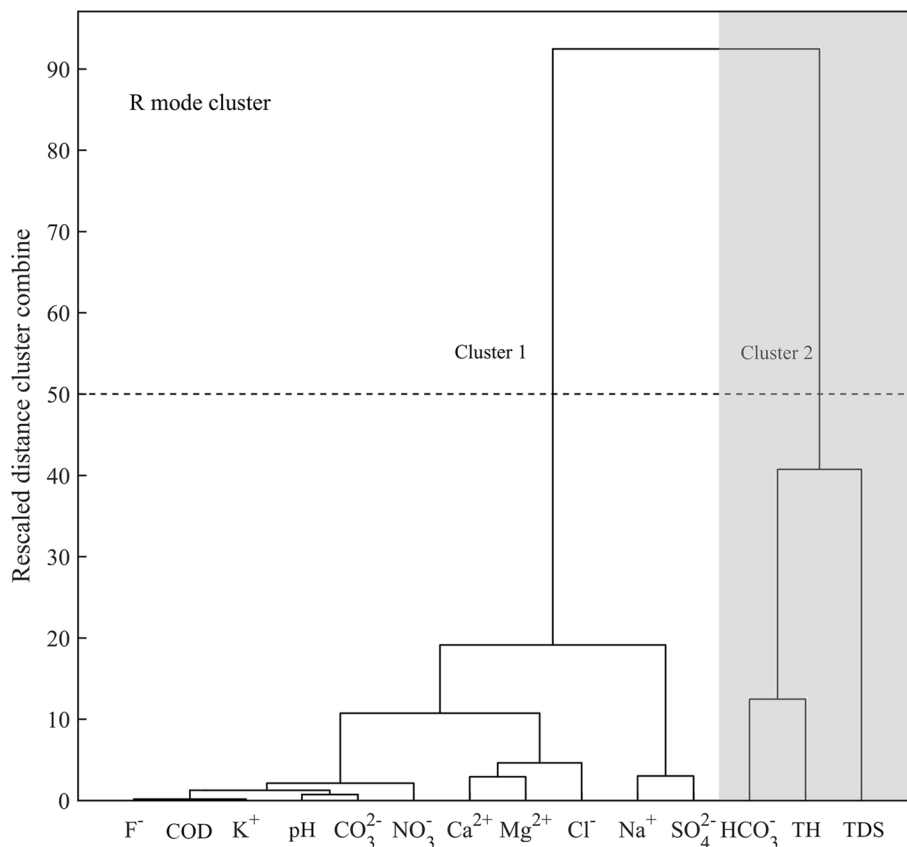
R mode HCA was used to the 14 water quality variables, and the results are shown in Fig. 7. Cluster 1 includes  $\text{F}^-$ , COD,  $\text{K}^+$ , pH,  $\text{CO}_3^{2-}$ ,  $\text{NO}_3^-$ ,  $\text{Ca}^{2+}$ ,  $\text{Mg}^{2+}$ ,  $\text{Cl}^-$ ,  $\text{Na}^+$ , and  $\text{SO}_4^{2-}$ . Cluster 2 includes  $\text{HCO}_3^-$ , TH, and TDS. In cluster 1, COD, pH, and  $\text{NO}_3^-$  are mainly influenced by human activities. The other physicochemical indices in cluster 1 are mainly controlled by a natural process, such as the dissolution of minerals and soil leaching. Therefore, cluster 1 represents the groundwater chemical characteristics regulated by both natural and anthropogenic processes. The indices in cluster

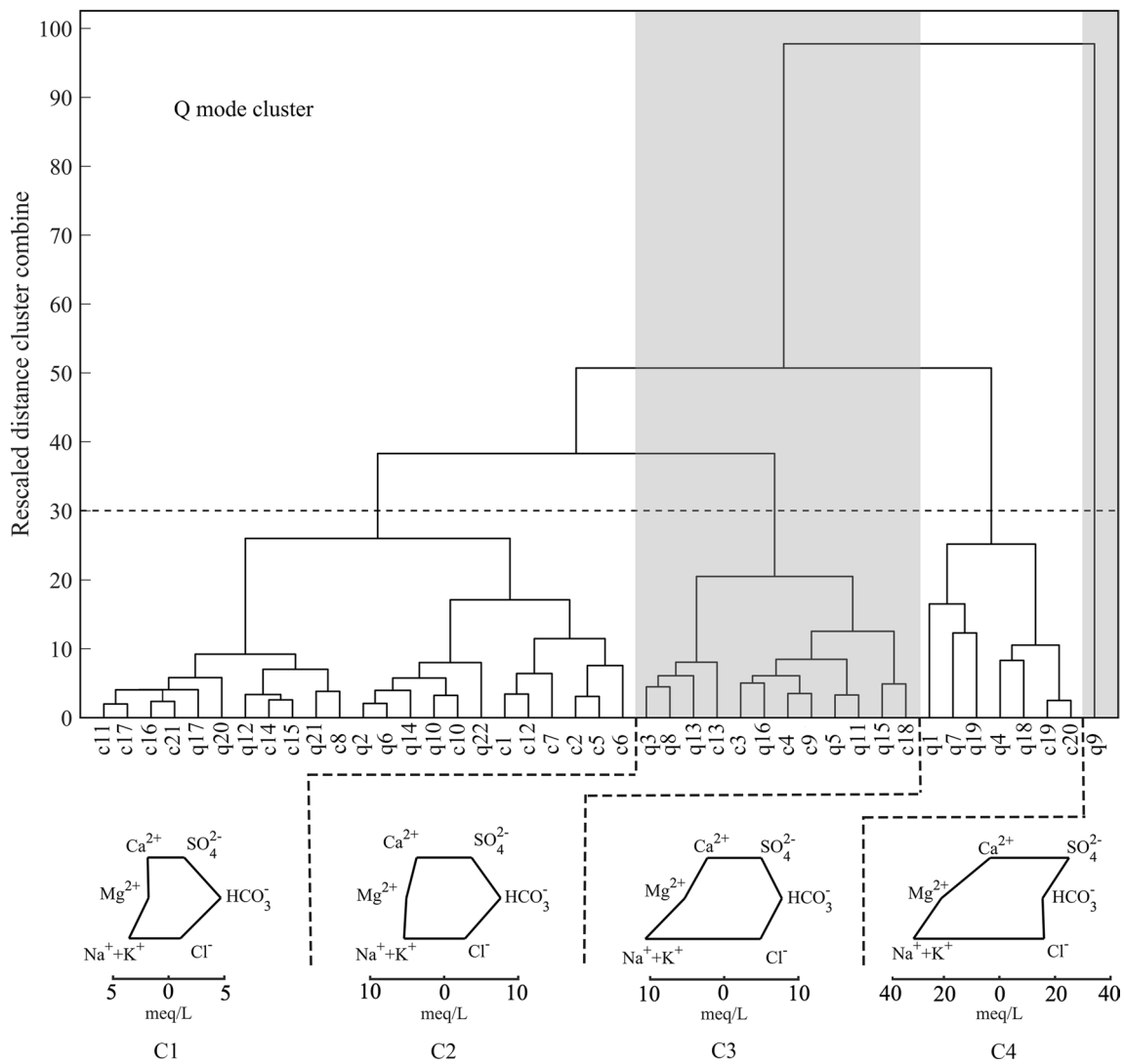
2 are related to major ions, which are mainly controlled by natural processes, such as dissolution of calcite, dolomite, gypsum, and fluorite.

Figure 8 shows the result of the Q mode HCA for the analysis of the 43 groundwater samples. In this study, a phenon line was drawn across the dendrogram at a linkage distance of approximately 30. This position of the phenon line allows a division of the dendrogram into four clusters of water samples (C1–C4). The Stiff diagrams of the four clusters based on median concentrations are also included in Fig. 8. To describe the characteristics of each cluster of samples, the median values for each parameter are presented in Table 4.

The dendrogram shows some indications of the level of similarity between the four clusters. C1 contains 23 samples, and C2 includes 12 samples. C1 and C2 are linked with a lower linkage distance compared to the other clusters, implying that they have a greater similarity. It can be inferred that C1 and C2 samples have the same or similar geochemical characteristics. C3 consists of seven groundwater samples, and C4 includes only one sample (q9). Weak similarities between the geochemistry of C4 and other cluster samples also are expected, because there is a large linkage distance between C4 and others. The Stiff diagrams (Fig. 8) and the data (Table 4) show that the four clusters are classified as disparate hydrochemical types. Samples from C1, C2, and

**Fig. 7** Dendrogram of R mode HCA of groundwater physicochemical indices





**Fig. 8** Dendrogram of Q mode HCA of groundwater samples and stiff diagram of each clusters

**Table 4** Concentration of parameters of different clusters

Parameters	C1	C2	C3	C4
pH	8.37	8.00	8.38	8.23
K <sup>+</sup>	1.55	1.98	1.96	9.50
Na <sup>+</sup>	81.10	123.42	243.71	706.00
Ca <sup>2+</sup>	37.82	74.64	45.68	66.21
Mg <sup>2+</sup>	21.99	62.09	64.98	254.30
F <sup>-</sup>	0.52	0.58	1.41	1.87
Cl <sup>-</sup>	37.47	99.50	173.14	569.20
SO <sub>4</sub> <sup>2-</sup>	66.91	177.44	239.69	1204.00
HCO <sub>3</sub> <sup>-</sup>	286.09	465.03	474.13	947.10
CO <sub>3</sub> <sup>2-</sup>	5.80	1.44	8.84	0.00
NO <sub>3</sub> <sup>-</sup>	2.77	19.80	39.31	107.20
TDS	458.17	785.67	1044.57	3400.00
COD	0.98	0.87	1.55	1.46
TH	185.08	442.16	385.99	1214.00

C3 are classified as HCO<sub>3</sub>-Na-K type and the concentrations of all ions except CO<sub>3</sub><sup>2-</sup> are lower than the sample from C4. The sample in C4 is classified as SO<sub>4</sub>-Na-K type and has a much higher concentration in SO<sub>4</sub><sup>2-</sup> compared with samples in other clusters. Most parameters except CO<sub>3</sub><sup>2-</sup>, pH, COD increase from C1 to C4.

Samples in C1 have the lowest ion concentrations, which may indicate that they did not have a long residence time within the geosphere, and their interactions with the surrounding minerals are not sufficient. This is confirmed by the box plot of the saturation index in Fig. 9, which shows that there is a slight increase in the saturation indices from C1 to C4. This might be due to the increasing water-rock interactions or by human activities. The trend in the saturation index implies that calcite and dolomite gradually become supersaturated, and fluorite and gypsum are close to saturation. The saturation indices of the minerals in C4 are higher

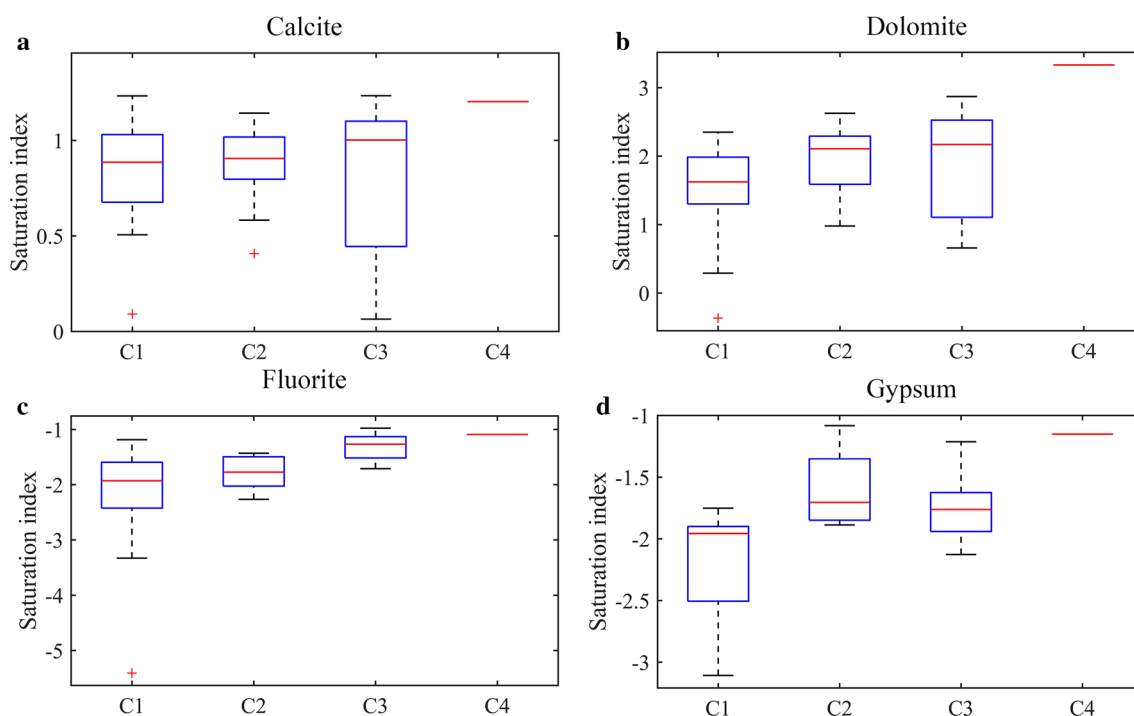


**Fig. 9** Box plot of **a** calcite, **b** dolomite, **c** fluorite, and **d** gypsum saturation indices

than those in the other clusters, which may be explained by a longer residence time and sufficient interaction with the surrounding minerals. The concentration of nitrate in C4 is 107.2 mg/L, indicating that the sample from C4 is significantly influenced by anthropogenic processes.

### Groundwater Management in the Guanzhong Basin

As presented earlier, the natural processes and human activities are regarded as the main influencing factors. On one hand, the anthropogenic processes can introduce more sulfate, nitrate, chloride, and organic matter into the groundwater, which influence the groundwater quality and human health. On the other hand, human activities can change the hydrogeological conditions, such as groundwater level, which may further change the hydrochemical characteristics. Considering the importance of Guanzhong Basin in the Belt and Road Initiative, it is urgent to adopt a sustainable groundwater quality management. Groundwater quality improvement programs should be conducted.

Weihe River, the biggest river running through the Guanzhong Basin, has close contact with local groundwater. However, wastewater produced by upstream industry and downstream domestic sewage have polluted the Weihe River. This will further affect the groundwater quality by through river water percolation. The local government should prevent the river water from further pollution and enhance the treatment of industrial wastewater and domestic sewage. In

addition, the rural toilet should be reformed to prevent the groundwater from pollution of bacteria, nitrate, and sulfate. Fertilizers and pesticides should be rationally used in the agricultural area, which will reduce the non-point source pollution. For areas with high fluoride and total hardness caused by natural factors, the government should organize tap water defluorination removal projects or install water purifiers to reduce potential human health risks. Meanwhile, the regular groundwater monitoring in the Guanzhong Basin is an indispensable part of groundwater management.

The groundwater quality is affected by multiple factors, including climate change, land use change, human activities, surface water percolation, and social development. The necessary step to ensure effective protection of groundwater is enhancing cooperation among different departments. Thus, groundwater research should be combined with natural sciences and social sciences, so that groundwater management can be more sustainable.

### Conclusions

The sources and influencing factors of groundwater quality in the central parts of the Guanzhong Basin were determined using hydrogeochemical, statistical and multivariate statistical techniques. We found that both natural and anthropogenic processes influence the groundwater chemistry. The findings can be summarized as follows:

- Most of the major ions in the groundwater are predominantly regulated by natural processes, as indicated by the correlation analysis. The chloralkaline indices demonstrate that cation exchange is a significant process influencing  $\text{Na}^+$  and  $\text{Ca}^{2+}$ . Sulfate and nitrate, however, are mainly influenced by anthropogenic processes, such as industrial and domestic effluents, elevated groundwater level due to irrigation.
- The extracted five VFs from factor analysis explain 89.366% of the total variance and are related to salinity, calcium ions, organics, nitrates, and carbonates, respectively. Overall, the salinity, calcium ion, and carbonate components are mainly controlled by natural processes. VF3 and VF4, however, represent anthropogenic processes. It should be noted that the anthropogenic and natural processes cannot completely be separated. Factor analysis is more effective in explaining the characteristics of groundwater hydrochemistry than principal component analysis in this study.
- R mode and Q mode HCA applied in this study. In the R mode HCA, cluster 1 represents the combination of natural and anthropogenic processes. Cluster 2 includes  $\text{HCO}_3^-$ , TH, and TDS, which are mainly governed by natural processes. Four geochemically distinct clusters can be classified by Q mode HCA. Samples from C1, C2, and C3 consist of  $\text{HCO}_3^-$ -Na-K or  $\text{HCO}_3^-$ -Na type samples, and the sample from C4 is of the  $\text{SO}_4$ -Na-K type. Sample from C4 comes from a phreatic aquifer, with high concentrations of major ions.
- Most of groundwater in the study area is generally suitable for multiple uses, except groundwater in a few locations. The usage of fertilizers and pesticides, and domestic and industrial wastewater could lead to negative influence on human health. Thus, continuous groundwater quality monitoring is necessary for sustainable groundwater quality management and protection. In further research, trace metals should be considered, and this will result in a more comprehensive understanding of groundwater quality.

**Acknowledgements** This work was financially supported by the National Natural Science Foundation of China (41761144059 and 42072286), the Fundamental Research Funds for the Central Universities of CHD (300102299301), the Fok Ying Tong Education Foundation (161098), the China Postdoctoral Science Foundation (2016M590911, 2015M580804, 2017T100719, and 2016T090878), the Shaanxi Postdoctoral Science Foundation (2016BSHTDZZ03 and 2015BSHTDZZ09), the Ten Thousand Talents Program (W03070125), and the Fundamental Research Funds for the Central Universities, CHD (300102290717). The editor and anonymous reviewers are acknowledged for their useful comments.

## Compliance with Ethical Standards

**Conflict of interest** The authors declare that they have no conflict of interest.

## References

- Adimalla N, Vasa SK, Li P (2018) Evaluation of groundwater quality, Peddavagu in Central Telangana (PCT), South India: an insight of controlling factors of fluoride enrichment. *Model Earth Syst Environ* 4:841–852. <https://doi.org/10.1007/s40808-018-0443-z>
- Bouchard DC, Williams MK, Surampalli RY (1992) Nitrate contamination of groundwater: sources and potential health effects. *J Am Water Works Assoc* 84(9):85–90. <https://doi.org/10.1002/j.1551-8833.1992.tb07430.x>
- Bu H, Tan X, Li S, Zhang Q (2010) Water quality assessment of the Jinshui River (China) using multivariate statistical techniques. *Environ Earth Sci* 60:1631–1639. <https://doi.org/10.1007/s12665-009-0297-9>
- Chen J, Wu H, Qian H, Li X (2018) Challenges and prospects of sustainable groundwater management in an agricultural plain along the Silk Road Economic Belt, north-west China. *Int J Water Resour Dev* 34(3):354–368. <https://doi.org/10.1080/07900627.2016.1238348>
- Cloutier V, Lefebvre R, Therrien R, Savard MM (2008) Multivariate statistical analysis of geochemical data as indicative of the hydrogeochemical evolution of groundwater in a sedimentary rock aquifer system. *J Hydrol* 353(3–4):294–313. <https://doi.org/10.1016/j.jhydrol.2008.02.015>
- Dar MA, Sankar K, Dar IA (2011) Fluorine contamination in groundwater: a major challenge. *Environ Monit Assess* 173:955–968. <https://doi.org/10.1007/s10661-010-1437-0>
- Fendorf S, Michael HA, van Geen A (2010) Spatial and temporal variations of groundwater arsenic in South and Southeast Asia. *Science* 328(5982):1123–1127. <https://doi.org/10.1126/science.1172974>
- Gorelick SM, Zheng C (2015) Global change and the groundwater management challenge. *Water Resour Res* 51(5):3031–3051. <https://doi.org/10.1002/2014wr016825>
- Han Z (2003) Ground water resources protection and aquifer recovery in China. *Environ Geol* 44:106–111. <https://doi.org/10.1007/s00254-002-0705-x>
- He S, Wu J (2019) Relationships of groundwater quality and associated health risks with land use/land cover patterns: A case study in a loess area, northwest China. *Hum Ecol Risk Assess* 25(1–2):354–373. <https://doi.org/10.1080/10807039.2019.1570463>
- He X, Wu J, He S (2019) Hydrochemical characteristics and quality evaluation of groundwater in terms of health risks in Luohe aquifer in Wuqi County of the Chinese Loess Plateau, northwest China. *Hum Ecol Risk Assess* 25(1–2):32–51. <https://doi.org/10.1080/10807039.2018.1531693>
- Hossain S, Hosono T, Yang H, Shimada J (2016) Geochemical processes controlling fluoride enrichment in groundwater at the Western Part of Kumamoto Area, Japan. *Water Air Soil Pollut* 227:385. <https://doi.org/10.1007/s11270-016-3089-3>
- Howard KWF, Howard KK (2016) The new “Silk Road Economic Belt” as a threat to the sustainable management of Central Asia’s transboundary water resources. *Environ Earth Sci* 75:976. <https://doi.org/10.1007/s12665-016-5752-9>
- Hu Y, Moiwo JP, Yang Y, Han S, Yang Y (2010) Agricultural water-saving and sustainable groundwater management in Shijiazhuang Irrigation District, North China Plain. *J Hydrol* 393(3–4):219–232. <https://doi.org/10.1016/j.jhydrol.2010.08.017>



- IAH (International Association of Hydrogeologists) (2015) World Water Day 2015—embracing groundwater. <https://iah.org/wp-content/uploads/2015/03/2015WWD.pdf>
- Kabir H, Gupta AK, Tripathy S (2019) Fluoride and human health: systematic appraisal of sources, exposures, metabolism, and toxicity. *Crit Rev Environ Sci Technol* 50(11):1116–1193. <https://doi.org/10.1080/10643389.2019.1647028>
- Li P, Qian H, Wu J, Ding J (2010) Geochemical modeling of groundwater in southern plain area of Pengyang County, Ningxia, China. *Water Sci Eng* 3(3):282–291. <https://doi.org/10.3882/j.issn.1674-2370.2010.03.004>
- Li P, Qian H, Wu J, Chen J (2013a) Sensitivity analysis of TOPSIS method in water quality assessment: I. Sensitivity to the parameter weights. *Environ Monit Assess* 185:2453–2461. <https://doi.org/10.1007/s10661-012-2723-9>
- Li P, Wu J, Qian H, Chen J (2013b) Sensitivity analysis of TOPSIS method in water quality assessment II: sensitivity to the index input data. *Environ Monit Assess* 185:2463–2474. <https://doi.org/10.1007/s10661-012-2724-8>
- Li P, Qian H, Wu J, Chen J, Zhang Y, Zhang H (2014) Occurrence and hydrogeochemistry of fluoride in alluvial aquifer of Weihe River, China. *Environ Earth Sci* 71:3133–3145. <https://doi.org/10.1007/s12665-013-2691-6>
- Li P, Qian H, Howard KWF, Wu J (2015a) Building a new and sustainable “Silk Road economic belt”. *Environ Earth Sci* 74:7267–7270. <https://doi.org/10.1007/s12665-015-4739-2>
- Li C, Gao X, Wang Y (2015b) Hydrogeochemistry of high-fluoride groundwater at Yuncheng Basin, northern China. *Sci Total Environ* 508:155–165. <https://doi.org/10.1016/j.scitotenv.2014.11.045>
- Li P, Wu J, Qian H (2016a) Hydrochemical appraisal of groundwater quality for drinking and irrigation purposes and the major influencing factors: a case study in and around Hua County, China. *Arab J Geosci* 9:15. <https://doi.org/10.1007/s12517-015-2059-1>
- Li P, Wu J, Qian H, Zhang Y, Yang N, Jing L, Yu P (2016b) Hydrogeochemical characterization of groundwater in and around a wastewater irrigated forest in the southeastern edge of the Tengger Desert, Northwest China. *Expo Health* 8:331–348. <https://doi.org/10.1007/s12403-016-0193-y>
- Li P, Tian R, Xue C, Wu J (2017) Progress, opportunities, and key fields for groundwater quality research under the impacts of human activities in China with a special focus on western China. *Environ Sci Pollut Res* 24:13224–13234. <https://doi.org/10.1007/s11356-017-8753-7>
- Li P, Qian H, Wu J (2018a) Conjunctive use of groundwater and surface water to reduce soil salinization in the Yinchuan Plain, Northwest China. *Int J Water Resour Dev* 34(3):337–353. <https://doi.org/10.1080/07900627.2018.1443059>
- Li P, He S, Yang N, Xiang G (2018b) Groundwater quality assessment for domestic and agricultural purposes in Yan’an City, northwest China: implications to sustainable groundwater quality management on the Loess Plateau. *Environ Earth Sci* 77:775. <https://doi.org/10.1007/s12665-018-7968-3>
- Li P, He X, Guo W (2019a) Spatial groundwater quality and potential health risks due to nitrate ingestion through drinking water: a case study in Yan’an City on the Loess Plateau of northwest China. *Hum Ecol Risk Assess* 25(1–2):11–31. <https://doi.org/10.1080/10807039.2018.1553612>
- Li P, He X, Li Y, Xiang G (2019b) Occurrence and health implication of fluoride in groundwater of loess aquifer in the Chinese loess plateau: a case study of Tongchuan, Northwest China. *Expo Health* 11:95–107. <https://doi.org/10.1007/s12403-018-0278-x>
- Liu C-W, Lin K-H, Kuo Y-M (2003) Application of factor analysis in the assessment of groundwater quality in a blackfoot disease area in Taiwan. *Sci Total Environ* 313(1–3):77–89. [https://doi.org/10.1016/S0048-9697\(02\)00683-6](https://doi.org/10.1016/S0048-9697(02)00683-6)
- Luo K, Zhang S, Tian Y, Gao X (2014) Arsenic distribution pattern in different sources of drinking water and their geological background in Guanzhong basin, Shaanxi, China. *Acta Geol Sin-Engl* 88(3):984–994. <https://doi.org/10.1111/1755-6724.12251>
- Panneer M, Sivakumar R, Senthilkumar M (2017) Fluoride hydrogeochemistry and its occurrence in drinking water in Morappur region of Dharmapuri District, South India. *Int J Environ Sci Technol* 14:1931–1944. <https://doi.org/10.1007/s13762-017-1277-3>
- Panneerselvam B, Paramasivam SK, Karuppannan S, Ravichandran N, Selvaraj P (2020) A GIS-based evaluation of hydrochemical characterization of groundwater in hard rock region, South Tamil Nadu, India. *Arab J Geosci* 13:837. <https://doi.org/10.1007/s12517-020-05813-w>
- Parkhurst DL, Appelo CAJ (1999) User’s guide to PHREEQC (version 2): a computer program for speciation, batch-reaction, one-dimensional transport, and inverse geochemical calculations. Water-resources investigations report 99-4259. US Geological Survey, Denver
- Piper AM (1944) A graphic procedure in the geochemical interpretation of water-analyses. *Trans Am Geophys Union* 25(6):914–928. <https://doi.org/10.1029/TR025i006p00914>
- Postigo C, Barcelo D (2015) Synthetic organic compounds and their transformation products in groundwater: occurrence, fate and mitigation. *Sci Total Environ* 503–504:32–47. <https://doi.org/10.1016/j.scitotenv.2014.06.019>
- Rodriguez-Lado L, Sun G, Berg M, Zhang Q, Xue H, Zheng Q, Johnson CA (2013) Groundwater arsenic contamination throughout China. *Science* 341(6148):866–868. <https://doi.org/10.1126/science.1237484>
- Schoeller H (1965) Qualitative evaluation of groundwater resources. In: *Methods and techniques of groundwater investigation and development*. Water Research Series 33: UNESCO, 54–83
- Schwarzenbach RP, Egli T, Hofstetter TB, von Gunten U, Wehrli B (2010) Global water pollution and human health. *Annu Rev Environ Resour* 35:109–136. <https://doi.org/10.1146/annurev-environ-100809-125342>
- Soujanya KB, Saxena PR, Kurakalva RM, Shankar K (2020) Evaluation of seasonal and temporal variations of groundwater quality around Jawaharnagar municipal solid waste dumpsite of Hyderabad city, India. *SN Appl Sci* 2:498. <https://doi.org/10.1007/s42452-020-2199-0>
- Sun G, Xu Y, Zheng Q, Xi S (2011) Arsenicosis history and research progress in Mainland China. *Kaohsiung J Med Sci* 27(9):377–381. <https://doi.org/10.1016/j.kjms.2011.05.004>
- Tao H, Tao FP, Liu WB (2013) Characteristics and influencing factors of groundwater dynamics in Guanzhong urban agglomeration during the last 50 years. *Hydrogeol Eng Geol* 40(6):37–42 + 61 (in Chinese). <http://doi.org/10.16030/j.cnki.issn.1000-3665.2013.06.017>
- Vega M, Pardo R, Barrado E, Luis D (1998) Assessment of seasonal and polluting effects on the quality of river water by exploratory data analysis. *Water Res* 32(12):3581–3592. [https://doi.org/10.1016/S0043-1354\(98\)00138-9](https://doi.org/10.1016/S0043-1354(98)00138-9)
- Wang W, Zhang Z, Duan L, Wang Z, Zhao Y, Zhang Q, Dai M, Liu H, Zheng X, Sun Y (2018) Response of the groundwater system in the Guanzhong Basin (central China) to climate change and human activities. *Hydrogeol J* 26:1429–1441. <https://doi.org/10.1007/s10040-018-1757-7>
- Ward M, Jones R, Brender J, De Kok T, Weyer P, Nolan B, Villanueva C, Van Breda S (2018) Drinking water nitrate and human health: an updated review. *Int J Environ Res Public Health* 15:1557. <https://doi.org/10.3390/ijerph15071557>
- Wu J, Li P, Qian H, Duan Z, Zhang X (2014) Using correlation and multivariate statistical analysis to identify hydrogeochemical processes affecting the major ion chemistry of waters: a case study

- in Laoheba phosphorite mine in Sichuan, China. *Arab J Geosci* 7:3973–3982. <https://doi.org/10.1007/s12517-013-1057-4>
- Wu J, Wang L, Wang S, Tian R, Xue C, Feng W, Li Y (2017) Spatiotemporal variation of groundwater quality in an arid area experiencing long-term paper wastewater irrigation, northwest China. *Environ Earth Sci* 76:460. <https://doi.org/10.1007/s12665-017-6787-2>
- Wu J, Li P, Wang D, Ren X, Wei M (2020) Statistical and multivariate statistical techniques to trace the sources and affecting factors of groundwater pollution in a rapidly growing city on the Chinese Loess Plateau. *Hum Ecol Risk Assess* 26(6):1603–1621. <https://doi.org/10.1080/10807039.2019.1594156>
- Zhang Y, Wu J, Xu B (2018) Human health risk assessment of groundwater nitrogen pollution in Jinghui canal irrigation area of the loess region, northwest China. *Environ Earth Sci* 77:273. <https://doi.org/10.1007/s12665-018-7456-9>
- Zhang Q, Xu P, Qian H (2019) Assessment of groundwater quality and human health risk(HHR) evaluation of nitrate in the central-western Guanzhong Basin, China. *Int J Environ Res Public Health* 16:4246. <https://doi.org/10.3390/ijerph16214246>
- Zhou Y, Wang Y, Du S, Zhang P, Zhang H, Zhang H (2018) Division and characteristics of groundwater system in Guanzhong Basin. *Geol Surv China* 5(4):67–75. <https://doi.org/10.19388/j.zgdzdc.2018.04.08> (in Chinese)
- Zhou Y, Ning J, Li L, Long Q, Wei A, Liu Z (2020a) Health risk assessment of groundwater in Gaobeidian, North China: distribution, source and chemical species of main contaminants. *Expo Health* 12:427–446. <https://doi.org/10.1007/s12403-020-00365-6>
- Zhou Y, Li P, Chen M, Dong Z, Lu C (2020b) Groundwater quality for potable and irrigation uses and associated health risk in southern part of Gu'an County, North China Plain. *Environ Geochem Health*. <https://doi.org/10.1007/s10653-020-00553-y>
- Zhou Y, Li P, Xue L, Dong Z, Li D (2020c) Solute geochemistry and groundwater quality for drinking and irrigation purposes: a case study in Xinle City, North China. *Geochemistry*. <https://doi.org/10.1016/j.chemer.2020.125609>